



**HAL**  
open science

## Engineering impacts on the Upper Rhine channel and floodplain over two centuries

Fanny Arnaud, Laurent Schmitt, Karen Johnstone, Anne-Julia Rollet, Hervé Piégay

► **To cite this version:**

Fanny Arnaud, Laurent Schmitt, Karen Johnstone, Anne-Julia Rollet, Hervé Piégay. Engineering impacts on the Upper Rhine channel and floodplain over two centuries. *Geomorphology*, 2019, 330, pp.13-27. 10.1016/j.geomorph.2019.01.004 . hal-02002992

**HAL Id: hal-02002992**

**<https://hal.science/hal-02002992v1>**

Submitted on 21 Oct 2021

**HAL** is a multi-disciplinary open access archive for the deposit and dissemination of scientific research documents, whether they are published or not. The documents may come from teaching and research institutions in France or abroad, or from public or private research centers.

L'archive ouverte pluridisciplinaire **HAL**, est destinée au dépôt et à la diffusion de documents scientifiques de niveau recherche, publiés ou non, émanant des établissements d'enseignement et de recherche français ou étrangers, des laboratoires publics ou privés.



Distributed under a Creative Commons Attribution - NonCommercial 4.0 International License

1           **Engineering impacts on the Upper Rhine channel and floodplain over two centuries**

2

3           Fanny Arnaud<sup>a,\*</sup>, Laurent Schmitt<sup>b</sup>, Karen Johnstone<sup>a</sup>, Anne-Julia Rollet<sup>c</sup>, Hervé Piégay<sup>a</sup>

4

5           <sup>a</sup> CNRS UMR 5600 EVS, University of Lyon/Site ENS, 15 parvis René Descartes, BP 7000 69342

6           Lyon Cedex 07, France

7           <sup>b</sup> University of Strasbourg, UMR 7362 LIVE, CNRS, ENGEES, 3 rue de l'Argonne, 67083 Strasbourg,

8           France

9           <sup>c</sup> CNRS UMR 6554 LETG - Rennes, University Rennes 2, Place du recteur Henri Le Moal, CS 24307

10          35043 Rennes Cedex, France

11          \* Corresponding author. Tel.: +33 4 37 37 65 40; E-mail: [fanny.arnaud@ens-lyon.fr](mailto:fanny.arnaud@ens-lyon.fr).

12

13          **Abstract**

14          The reconstruction of long-term (>100 yr) channel changes is critical to understanding how natural and  
15          anthropogenic factors impact the evolution of river systems. It provides information on channel  
16          sensitivity and the limitations for channel repair in a functional river restoration context. This study  
17          presents a two-century analysis of the evolution of a large braided and anabranching river, the Upper  
18          Rhine downstream of Basel, which has experienced three phases of engineering works (nineteenth  
19          century channelization, 1930s groyne construction, and 1950s damming and by-passing). We studied  
20          historical maps, longitudinal profiles, and cross sections to investigate changes in the areas and  
21          geometries of fluvial features from 1828 to 2009. The results showed a drastic floodplain drying out  
22          following nineteenth century channelization (93% reduction of fully connected channels, 48%  
23          augmentation of partially connected channels, augmentation of disconnected water bodies by more  
24          than five times, and augmentation of terrestrialized channels of more than two times; 1828–1925).  
25          Changes propagated downstream at 280 m yr<sup>-1</sup> on the 50-km long river continuum. The channel  
26          exhibited bed topography of large forms in 1880, with a median pool-riffle amplitude of 4.0 m, locally  
27          reaching 6.6 m. Among the three phases of engineering works on the Upper Rhine, channelization  
28          had the most impact on planform (floodplain terrestrialization) and vertical (7 cm yr<sup>-1</sup> bed degradation)  
29          adjustments, with short reaction times and effects lasting several decades. Damming had the greatest  
30          impact on peak flows, and can explain the lower magnitude of the channel changes in the

31 contemporary period. We synthesized the complex cause-effect relationships between  
32 natural/anthropogenic controlling factors and hydromorphological processes over the past 200 yr, and  
33 outlined the evolutionary trend of the main geomorphic variables, which can be used as a knowledge  
34 framework to evaluate future morphodynamic restoration schemes.

35

## 36 **Keywords**

37 Upper Rhine; Controlling factors; Channelization; Evolutionary trajectory; Braided river; Anabranching  
38 river.

39

## 40 **1. Introduction**

41 The morphological and ecological consequences of human activity on river channels and floodplains  
42 over the last 200 yr have been well documented. One of the direct and most dramatic modifications is  
43 channelization, which includes all engineering procedures that either straighten, embank, enlarge, or  
44 protect an existing channel, or that involve the creation of new channels (Brookes, 1988). Systematic  
45 river channelization works were applied in the mid- and late nineteenth century in Europe and  
46 elsewhere to satisfy demands for flood control, drainage improvement, or maintenance of navigation  
47 (Downs and Gregory, 2004; Herget et al., 2005; Gregory, 2006). These works have resulted in drastic  
48 landscape transformations, from multiple river channels to single-thread channel configurations, as  
49 experienced in the Danube (Pišút, 2002; Hohensinner et al., 2011), the Rhône (Bravard et al., 1986;  
50 Provansal et al., 2014), the Rhine (Hudson et al., 2008), Italian rivers (Surian and Rinaldi, 2003), and  
51 braided rivers of the French Alps (Piégay et al., 2009).

52 A major consequence of straightened channels is riverbed degradation, which occurs with a short  
53 reaction time, and can reach several meters in depth in some cases (Brookes, 1988; Surian and  
54 Rinaldi, 2003; Hudson et al., 2008). Bed degradation can induce lowering of the adjacent groundwater  
55 level, with a subsequent loss of river-floodplain connectivity and a tendency towards floodplain  
56 terrestrialization (Bravard et al., 1999; Girel et al., 2003). Dikes (levees) themselves alter the lateral  
57 connectivity by closing side channels, which leads to channel abandonment (Bravard et al., 1986;  
58 Peiry, 1986; Dépret et al., 2017). Some studies have revealed the magnitude of change in  
59 anabranching channel types following channelization (Hohensinner et al., 2004; Diaz-Redondo et al.,  
60 2017), but the patterns of change have only rarely been detailed along a downstream continuum

61 (Gregory et al., 2002). Additionally, many channelized rivers have undergone further engineering in  
62 the twentieth century (e.g., hydropower dams and gravel mining), which have further complicated their  
63 evolutionary trajectory (Surian and Rinaldi, 2003; Provansal et al., 2014; Ziliani and Surian, 2016).  
64 Understanding the history of multi-impacted rivers over fine spatio-temporal scales is a major  
65 challenge in the context of current river restoration. Geomorphic diagnosis provides information on  
66 channel sensitivity and the limitations for channel repair. By defining realistic goals that integrate both  
67 reversible and irreversible changes for recovering a set of targeted river dynamics, rather than a static  
68 past reference state, it permits selection of the most efficient and sustainable restoration  
69 configurations (Dufour and Piégay, 2009). Exploration of the functional trajectories of change should  
70 also be useful for anticipating responses after restoration, by assessing the potential benefits and  
71 limitations for channel repair (Mika et al., 2010). However, the integration of long-term (>100 yr)  
72 channel change analysis into functional restoration projects remains rare (Bravard and Gaydou, 2015;  
73 Eschbach et al., 2018; Scorpio et al., 2018).

74 This study aims to quantify the morphological effects of channelization and further engineering works  
75 on a braided and anabranching river system over substantial temporal (181 yr) and spatial (50-km long  
76 reach) scales. The research was conducted on the Upper Rhine River, which is a major  
77 environmental, cultural, and socio-economic corridor in Europe. Channelization of the river started in  
78 1817, which makes it one of the first intensive large-scale engineering schemes undertaken on a large  
79 river anywhere in the world (Tricart and Bravard, 1991; Uehlinger et al., 2009). The contemporary  
80 hydromorphological evolution (1930s-2010s) was quantified for a downstream continuum, the 50-km-  
81 long *Old Rhine* downstream of Basel, by Arnaud et al. (2015). This study provided insights into the  
82 process-based restoration of the river reach. The present study integrates this medium-term  
83 geomorphic analysis and future restoration schemes with the long-term temporal trajectory (1828 to  
84 2009). We aim to specify the spatio-temporal patterns of planform and vertical channel changes by  
85 responding to the following questions: What was the channel pattern and what were the dynamics  
86 prior to channelization? How did channelization affect processes and forms in terms of response times  
87 and magnitudes? What is the relative importance of channelization effects compared to the 1930s and  
88 1950s engineering effects? What are the implications for functional river restoration?

89 This study combines a quantitative and qualitative analysis to outline the evolutionary trajectories of  
90 some of the main geomorphic variables of the fluvial system (active-channel width, bed level, channel

91 types) over a continuous time period of almost 200 yr. The multi-century material provides new and  
92 complementary information to the multi-decade study by Arnaud et al. (2015). In particular, historical  
93 maps, longitudinal profiles, and cross sections provide an accurate description of the channel pattern  
94 before and after engineering works. Some aspects of channel evolution and restoration issues in the  
95 upstream part of the Upper Rhine could be in common with other large braided/anabranching multi-  
96 impacted rivers worldwide.

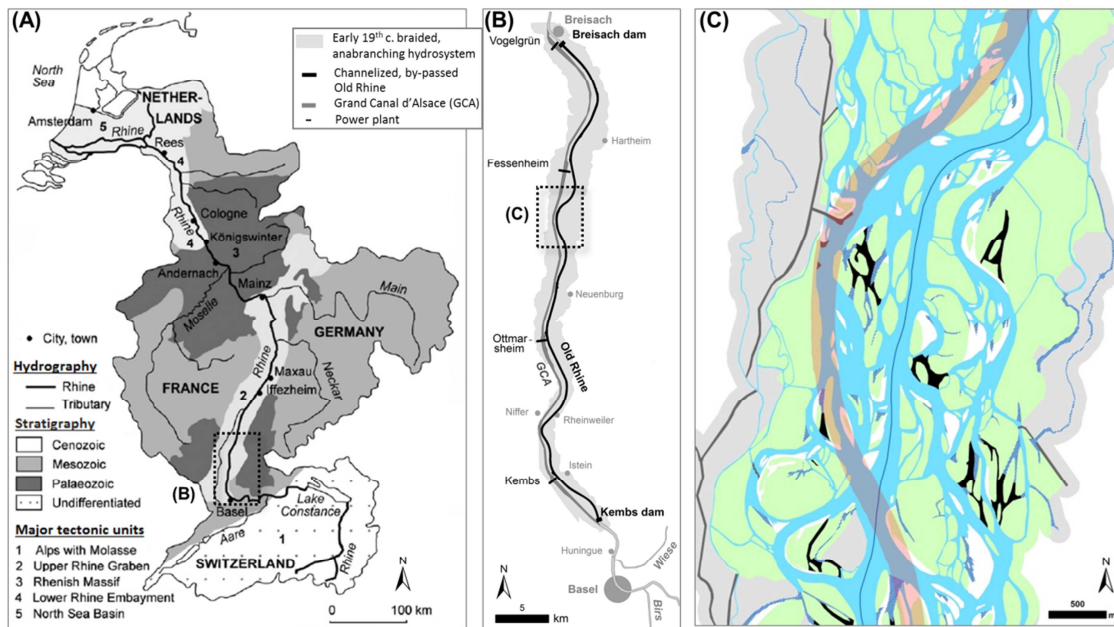
97

## 98 **2. Study area**

99 The 50-km long reach discussed in this study is located between Kembs (kilometric post [KP] 174.0)  
100 and Breisach (KP 224.8). This reach lies at the southern and upstream part of the Upper Rhine  
101 Graben, which is a 310-km long and 35-km wide spectacular subsidence zone within the European  
102 Rift system (Fig.1A; Uehlinger et al., 2009). The Upper Rhine Graben consists of Mesozoic strata with  
103 an overlying cover of marine sandy-clayey Tertiary material of more than 2000 m in depth (CHR,  
104 2009). The top cover between Basel (KP 170.0) and Breisach is a large alluvial fan, which is in places  
105 up to 250-m thick, and was formed during the Last Glaciation of the Alps ( $\approx 20$  ka BP) and the Younger  
106 Dryas (13-11 ka BP). In this reach, the sediments originate from the northern Swiss Alps, the Swiss  
107 Molasse Basin, and the Jura Mountains (Kock et al., 2009). After the Younger Dryas, the longitudinal  
108 profile of the Upper Rhine adjusted to changes in the controlling variables of the fluvial system: (1) a  
109 decrease in the water and sediment flux following the Holocene warming (Schmitt et al., 2016), (2)  
110 sediment trapping in lakes formed after the retreat of the Rhine Glacier area and which control 60% of  
111 the river network upstream of Basel (Walser, 1959), and (3) neotectonics, notably an uplift of the  
112 Upper Rhine Graben upstream from Mulhouse and a subsidence downstream (Nivière et al., 2006;  
113 Schmitt et al., 2016). These resulted in erosion of the alluvial fan down to a depth of 30 m (Kock et al.,  
114 2009; Schmitt et al., 2016).

115 The early nineteenth century Upper Rhine downstream of Basel can be classified as a gravel-  
116 dominated, braided (Carbiener and Schnitzler, 1990), and anabranching (Nanson and Knighton, 1996;  
117 Herget et al., 2005; Schmitt et al., 2016) river (Fig. 1C). Farther downstream, the Upper Rhine  
118 exhibited a progressively anabranching (mainly anastomoses; downstream of Breisach) and  
119 meandering (downstream of Strasbourg) river pattern (Carbiener and Schnitzler, 1990; Diaz-Redondo  
120 et al., 2017). Schmitt et al. (2016) showed that the longitudinal bed slope variation and the Holocene

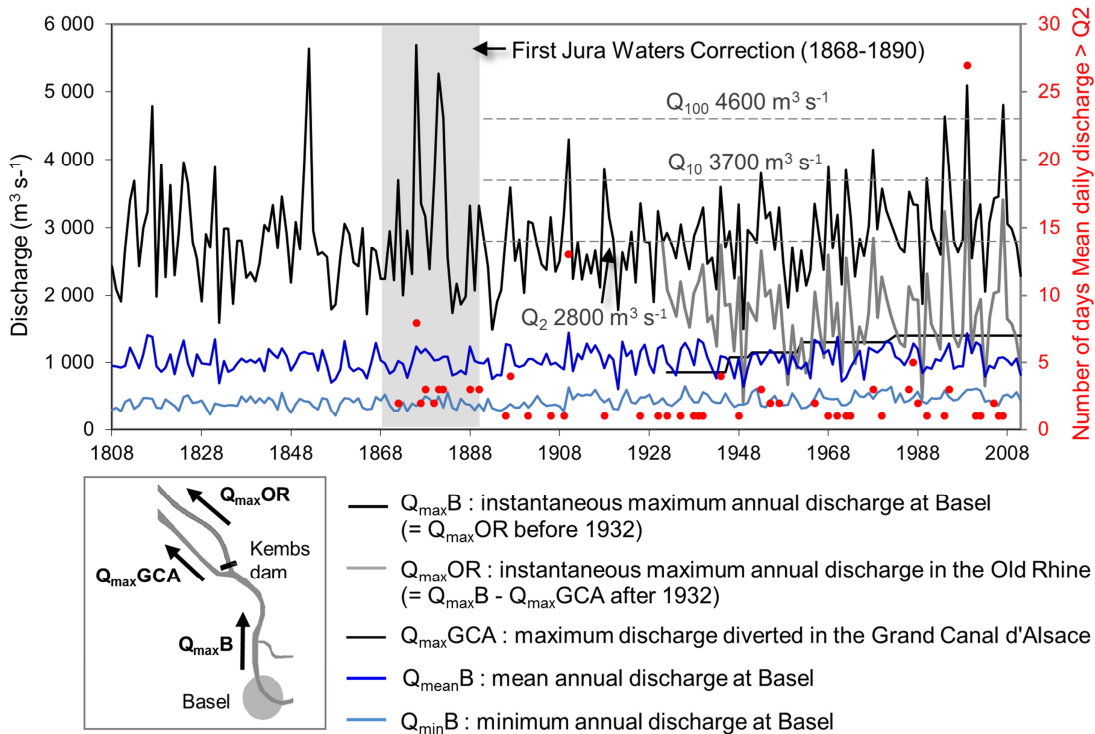
121 bed-level evolution were the two discriminating variables explaining the longitudinal geomorphic  
 122 continuum of the pre-channelized Upper Rhine.



123  
 124 Fig. 1. (A) Geologic-tectonic setting of the Rhine basin (after Frings et al., 2014). (B) Extent of the  
 125 early nineteenth century complex channel area, the present Old Rhine and the Grand Canal d'Alsace.  
 126 (C) The 1828 cartography for a section near Blodelsheim showing the complex braided and  
 127 anabranching system (see feature legend in Fig. 3). The thalweg is the blue line and the planned  
 128 position of the 200-m wide channelized river is mapped in red.

129  
 130 Discharge measurements started in 1808 in Basel, which makes for one of the longest uninterrupted  
 131 hydrological series in Europe (Wetter et al., 2011). The *First Jura Waters Correction Project* (1868-  
 132 1890) in the upstream Swiss basin diverted the Aare River to Lake Biel to dry up the floodplain for  
 133 agricultural development and delay flood peaks at the confluence with the Emme (Wetter et al., 2011).  
 134 These engineering works substantially modified the downstream flow regime, so that the  
 135 contemporary hydrology of the Upper Rhine is usually analyzed as starting in 1891 (CECR, 1978). The  
 136 mean annual discharge at the Basel gauging station over the period 1891–2011 is  $1050 \text{ m}^3 \text{ s}^{-1}$ , and  
 137 the 2-, 10- and 100-yr flood discharges are  $\sim 2800$ ,  $3700$ , and  $4600 \text{ m}^3 \text{ s}^{-1}$ , respectively. The top three  
 138 major floods recorded in Basel since 1808 occurred in the nineteenth century in September 1852  
 139 ( $5640 \text{ m}^3 \text{ s}^{-1}$ ), June 1876 ( $5700 \text{ m}^3 \text{ s}^{-1}$ ), and September 1881 ( $5280 \text{ m}^3 \text{ s}^{-1}$ ; Fig. 2). Three recent major  
 140 floods have occurred since the 1990s, with discharges of 4640, 5090, and  $4810 \text{ m}^3 \text{ s}^{-1}$  recorded in

141 May 1994, May 1999, and August 2007, respectively (top seven major floods recorded in Basel since  
 142 1808). The number of days that the mean daily discharge exceeded the 2-yr flood discharge varied  
 143 between 0 and 27 days per year (1869–2011; Fig. 2; discharge information from Ghezzi (1926) and  
 144 the Swiss Federal Office for the Environment).



145 Fig. 2. Maximum, mean, and minimum annual discharge series at Basel and in the Old Rhine for the  
 146 period 1808–2011. The discharge diverted into the Grand Canal d'Alsace was progressively increased  
 147 between 1932 and 1983, from 850 to 1400 m<sup>3</sup> s<sup>-1</sup>, to support growing navigation traffic and  
 148 hydroelectricity requirements. Red points indicate the number of days per year that the mean daily  
 149 discharge exceeded the 2-yr flood discharge.

150

151 Over centuries, the growing population in the Upper Rhine floodplain took protective measures against  
 152 the shifting river. The first artificial meander cuts date from the fourteenth century, but the effect of  
 153 such actions was localized and did not affect the natural river dynamics (Uehlinger et al., 2009). The  
 154 nineteenth century channelization belongs to the period of systematic stabilization of large rivers in  
 155 Europe, performed on a regional instead of a local scale (Herget et al., 2005). Channelization was  
 156 conducted on the study reach between 1842 and 1876 following the plans of the Badenese hydraulic  
 157 engineer J.G. Tulla (1825). The primary objectives were to narrow and shorten the river course to

158 cause bed degradation and subsequently reduce overflowing, and to provide flood control, border  
159 fixation, navigation improvement, and assist agriculture. The 3.5-km wide complex channel system  
160 was changed into a 200-m wide channelized river (Fig. 1C) by the construction of dikes (levees) over  
161 600 to 900 m longitudinal sections. The 50-m long intervals between these sections allowed major  
162 floods to exit to high-flow dikes built several hundred meters behind. In the 1920s, bed degradation at  
163 Istein (KP 178.0) reached the Jurassic limestone substratum, thus forming rapids on the bedrock  
164 outcrop, and impeding navigation between Germany and Switzerland (Humbert and Descombes,  
165 1985; Tricart and Bravard, 1991). Regularization works were then conducted from 1931 to 1939  
166 following the plans of the Badenese engineer M. Honsell, inspired by works by H. Girardon on the  
167 Rhône and M. Fargue on the Garonne (Humbert and Descombes, 1985). Lateral groyne fields were  
168 constructed downstream from the Istein bedrock outcrop to create a 75-m wide shipping channel  
169 under a sinusoidal pattern assumed to stabilize the longitudinal profile (Schneider, 1966). Finally,  
170 damming (1932) and construction of the Grand Canal d'Alsace (1932 to 1959) were aimed at  
171 hydropower generation and navigation improvement. The Kembs Dam conveys most of the flow  
172 (maximum discharge:  $1400 \text{ m}^3 \text{ s}^{-1}$ ) into a lateral canal that supplies the power plants of Kembs,  
173 Ottmarsheim, Fessenheim, and Vogelgrün (Fig. 1B). A minimum flow ( $50\text{--}150 \text{ m}^3 \text{ s}^{-1}$ ) is maintained in  
174 the by-passed Old Rhine for 81% of the time (Arnaud et al., 2015).

175

### 176 **3. Material and methods**

177 Planform changes over the period 1828–1925 were investigated for the 3.5-km wide hydrosystem  
178 area. This area (12,629 ha) was delimited by the farthest side channels connected upstream and  
179 downstream prior to channelization (1828), with a 100-m buffer applied (Fig. 1C). Vertical changes  
180 over the period 1880–2009 were investigated in the 200-m wide single-thread channel.

181

#### 182 *3.1. Planform data*

183 Two maps constructed before channelization (1828, 1838), one constructed towards the completion of  
184 channelization (1872), and one constructed fifty years later (1925) were identified (Table 1). The 1828  
185 and 1838 editions (1:20,000) were produced for the planning of river channelization and to map the  
186 changing French-German border. Thus, they are considered as more detailed descriptions of the  
187 Upper Rhine fluvial and riverine landscape in comparison with former editions (e.g., Cassini maps;

188 Bravard and Bethemont, 1989). Fewer features and less detailed delineation are presented on the  
 189 1872 (1:20,000) and 1925 (1:25,000) maps (Fig. 3). The maps were not accurately dated, but as their  
 190 purpose was to define international borders and river engineering, the mapped aquatic channel was  
 191 assumed to represent the mean discharge, as is usual in cartography (Diaz-Redondo et al., 2017).  
 192 The 1828 and 1925 maps were rectified to a 2008 orthophotograph using ArcMap v.10.1. The 1838  
 193 and 1872 maps were rectified to the 1828 map sheets using triangulation posts mapped on each  
 194 sheet. The resulting root mean square error (RMSE) ranged from 6.8 to 19.0 m per map sheet.

Year	Type	Source	Legend information	Scale	Number of sheets	RMSE max (m)	Discharge ( $\text{m}^3 \text{s}^{-1}$ ) <sup>a</sup>
1828	BW	BNU	Y	1:20,000	6	17.1	990
1838	C	PCA	N	1:20,000	6	6.8	1000
1872	C	PCA	N	1:20,000	6	14.5	1020
1925	C	Arch. Dép. 68	Y	1:25,000	4	19.0	810

195 Table 1. Maps used in the planform analysis.

196 BW: black and white; C: colored. Y: legend available; N: no legend. RMSE: root mean square error.  
 197 BNU: Bibliothèque Nationale et Universitaire de Strasbourg; PCA: Petite Camargue Alsacienne; Arch.  
 198 Dép. 68: Archives Départementales du Haut-Rhin.

199 <sup>a</sup> Source: before 1869, Ghezzi (1926); after 1869, Swiss Federal Office for the Environment.

200

201 Natural and artificial water bodies, unvegetated gravel/sand bars, vegetation boundaries,  
 202 terrestrialized channels, and anthropogenic features (croplands/villages/roads, dikes/embankments)  
 203 on the 1828, 1872 and 1925 maps were digitized at a 1:5000 scale. Differences in form, position,  
 204 color, texture, and legend information were used when available (Fig. 3). Natural water bodies were  
 205 subclassified into three channel types according to their hydrological connectivity (Gregory et al.,  
 206 2002; Hohensinner et al., 2004; Diaz-Redondo et al., 2017): fully connected channels (including the  
 207 mainstem, side channels, and tributaries), partially connected channels (channels connected only at  
 208 the upstream or downstream end, including backwaters) and fully disconnected water bodies (oxbow  
 209 lakes). Terrestrialized channels are former channels that are now full of sediments. Terrestrialization,  
 210 i.e., the passage from the aquatic to the terrestrial stage, could have occurred according two main  
 211 processes: filling by coarse and fine sediment deposits, and/or lowering of the water level resulting  
 212 from main channel incision (Bornette et al., 1996; Dépret et al., 2017).

213 The delineation of features on the 1925 map was not as accurate as previous editions, and the legend  
214 colors (e.g., blue for water bodies) and symbols (e.g., vegetated areas) were not systematically  
215 applied to the different sheets. This could induce errors in the identification of features, e.g., connected  
216 and disconnected channels could be confused, or terrestrialized channels could be mistaken for  
217 roads, dikes, or vegetation. Retro-interpretation from the 1925 to 1828 maps helped distinguish some  
218 features with respect to the river-floodplain succession stages.

219 Assessment of the early nineteenth century lateral channel migration was based on the thalweg  
220 comparison in 1828 and 1838 for 5-km long channel segments, i.e., half a map sheet ( $n = 11$ ).

221 Channel sinuosity was calculated using the same 5-km long channel segments of the thalwegs of  
222 1828 and 1838, and the channelized river centerline of 1872, with the three dates being compared  
223 with the 1828 hydrosystem centerline. The lateral distributions of the channel types based on three  
224 cross sections located on the upstream (KP 179.5), middle (KP 197), and downstream (KP 216.5)  
225 sections of the river reach were also analyzed. On these cross sections, the number of channels,  
226 channel width, and distance to the channelized river centerline were calculated for the three dates.

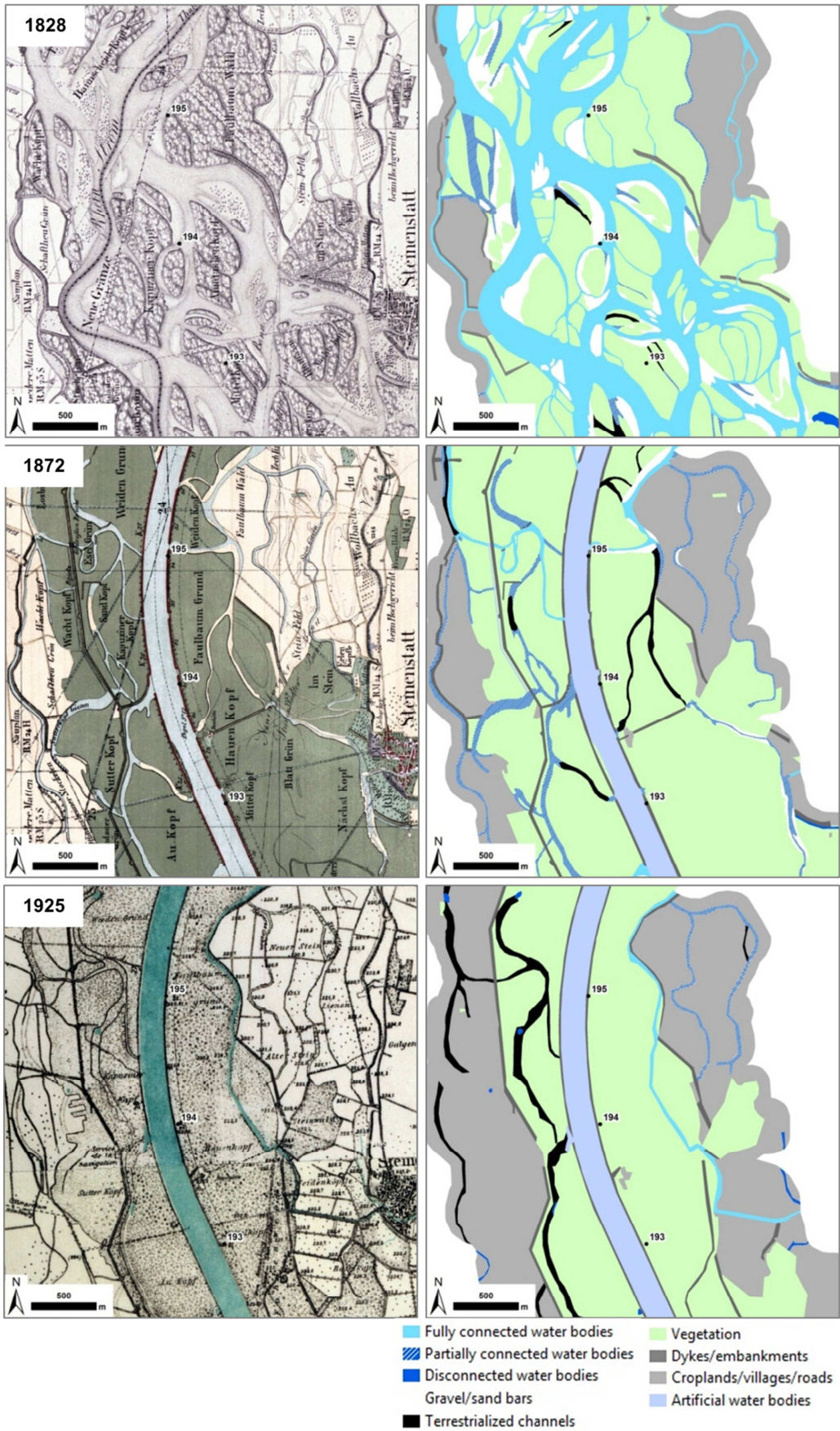
227 The longitudinal patterns of change in channel type areas were detailed by extracting areas for 500-m  
228 long channel segments ( $n = 99$ ) and calculating the differences per period. Homogeneous subreaches  
229 were statistically delineated using the “Hubert test” tool of the *FluvialCorridor* toolbox developed by  
230 Roux et al. (2015). The Hubert test for stationarity (Hubert, 2000) is especially successful for  
231 identifying longitudinal discontinuities on univariate series. It provides subreach segmentation when  
232 the difference of the mean between two consecutive segments is significant. Then, the overall  
233 propagation rate of channel changes ( $R$ , in  $\text{m y}^{-1}$ ) was calculated as:

234 
$$R = \frac{(\sum_{i=1}^n \overline{KP_{P_2}} - \overline{KP_{P_1}}) \times 1000}{4 \times P_2} \quad (1)$$

235 where  $\overline{KP_{P_2}}$  is the mean kilometric point of subreaches where the highest changes in channel type  
236 area occurred during the period  $P_2$  (1925–1872; 53 yr), the period  $P_1$  is 1872–1828, and  $n$  is the  
237 number of channel types ( $n = 4$ : fully connected, partially connected, fully disconnected, terrestrialized  
238 channels).

239

240 Finally, rates of change in active-channel width (sum of connected channels and unvegetated gravel  
241 bars) pre- and post-channelization were compared with the post-damming period (1950-2008) using  
242 the dataset reported in Arnaud et al. (2015).



244 Fig. 3. Examples of feature delineation on three old maps.

245

### 246 3.2. Topographic data

247 We compared from 197 to 240 thalweg points to determine trends of bed-level changes on the 50-km  
 248 long study reach. Thalweg profiles were compiled for five dates from 1880 to 2009 (Table 2); for 1880  
 249 (a few years after the completion of channelization), 1935 (during the regularization and three years  
 250 after damming and by-passing of the upstream part of the study reach), 1950–56 (during the by-  
 251 passing scheme), 1985–93, and 2009 (after by-passing). The three most recent thalweg profiles were  
 252 extracted from the cross-section series reported in Arnaud et al. (2015). These cross sections were  
 253 surveyed every 200 m and at the same location on each of the three dates. The historical paper  
 254 documents from 1880 and 1935 describe the thalweg profile under a continuous line from upstream to  
 255 downstream. As kilometric posts are located on the right (German) dike of the channelized river and  
 256 their position had not changed since the nineteenth century, we could apply the same 200-m spacing  
 257 to the historical profiles. Bed-level comparisons were possible after adjustment of the historical vertical  
 258 datum to the current vertical datum (Table 2; vertical datum information from R. Ostermann and H.  
 259 Lehmacher, Regierungspräsidium Freiburg, 2010).

Year	Type	Source	Covered reach (kilometric post)	Space interval	Number of surveys	Vertical datum	Vertical adjustment to NN n.S. <sup>a</sup>
1880	L	WSA	174.1–220.8	~ 1 point per 200 m	233 points	AP	+ 10 cm
1935	L	SNS	178.0–220.8	~ 1 point per 200 m	213 points	DHHN12	+ 11 cm
1950–56	L	WSA	174.4–179.8 (1950–56) 180.04–194.4 (1950–52) 194.61–214.0 (1952–56)	~ 1 point per 200 m	197 points	NN n.S.	
1985–93	L	WSA	174.4–179.8 (1985) 180.04–209.93 (1993) 210.0–220.8 (1985)	~ 1 point per 200 m	231 points	NN n.S.	
2009	L	WSA	174.1–220.8	~ 1 point per 200 m	240 points	NN n.S.	
1884	CS	Arch. Dép. 68	174.0–218.0	~ 1 CS per 3 km	21 CS	*	
1923	CS	Arch. Gén. Karlsruhe	178.0–182.0 196.0–198.0	~ 1 CS per 100 m	60 CS	**	
1930–37	CS	WSA	178.8–218.0	~ 1 CS per 3 km	14 CS	DHHN12	+ 11 cm
1950–56	CS	WSA	175.6–213.0	~ 1 CS per 3 km	14 CS	NN n.S.	
1985–93	CS	WSA	175.6–178.8 (1985) 182.91–205.82 (1993) 211.4–218.0 (1985)	~ 1 CS per 3 km	14 CS	NN n.S.	
2009	CS	WSA	175.6–218.0	~ 1 CS per 3 km	14 CS	NN n.S.	

260 Table 2. Topographic data used in the vertical analysis.  
261 L: longitudinal profile (thalweg); CS: cross-sectional profile; WSA: Wasser- und Schifffahrtsamt  
262 Freiburg; SNS: Service de la Navigation de Strasbourg; Arch. Gén.: Archives Générales; AP:  
263 Amsterdamer Pegel; DHHN12: Deutsches Haupthöhennetz 1912; NN n.S.: Normal Null neues  
264 System; \* bed level relative to the low-flow water level; \*\* no bed-level information; <sup>a</sup> Mean values of  
265 vertical datum differences between Basel and Breisach.

266  
267 Riffles and pools were identified from a linear regression fitted to the thalweg profiles; the maximum-  
268 size residuals above the regression line identifying riffles, and the minimum-size residuals identifying  
269 pools (Vetter, 2011). The median amplitude and spacing of pool-riffle sequences were calculated, as  
270 well as the ratio D/W, with D as the pool-to-pool spacing, and W as the median active-channel width  
271 between dikes (W = 209 m in 1880 and 1935; W = 153, 110, and 111 m in the 1950s, 1990s, and  
272 2010s, respectively; see Fig. 4C).

273 Six cross-section series were also compared (Table 2). The spacing of the surveys in 1884 was  
274 approximately 2000 m ( $n = 21$ ), while in 1923 it was 100 m ( $n = 60$ ). Bed-level information was given  
275 relative to the low-flow water level (1884), or no bed-level information was given (1923). These cross  
276 sections were analyzed qualitatively to determine channel geometry, especially the presence of lateral  
277 bars and islands. Changes in channel geometry after regularization and damming were quantified by  
278 comparing 14 cross sections performed between 1930 and 2009 (Table 2). These were selected  
279 according to a relatively constant spacing on the study reach (~3000 m). Atypical geometries in  
280 comparison with adjacent cross sections were excluded.

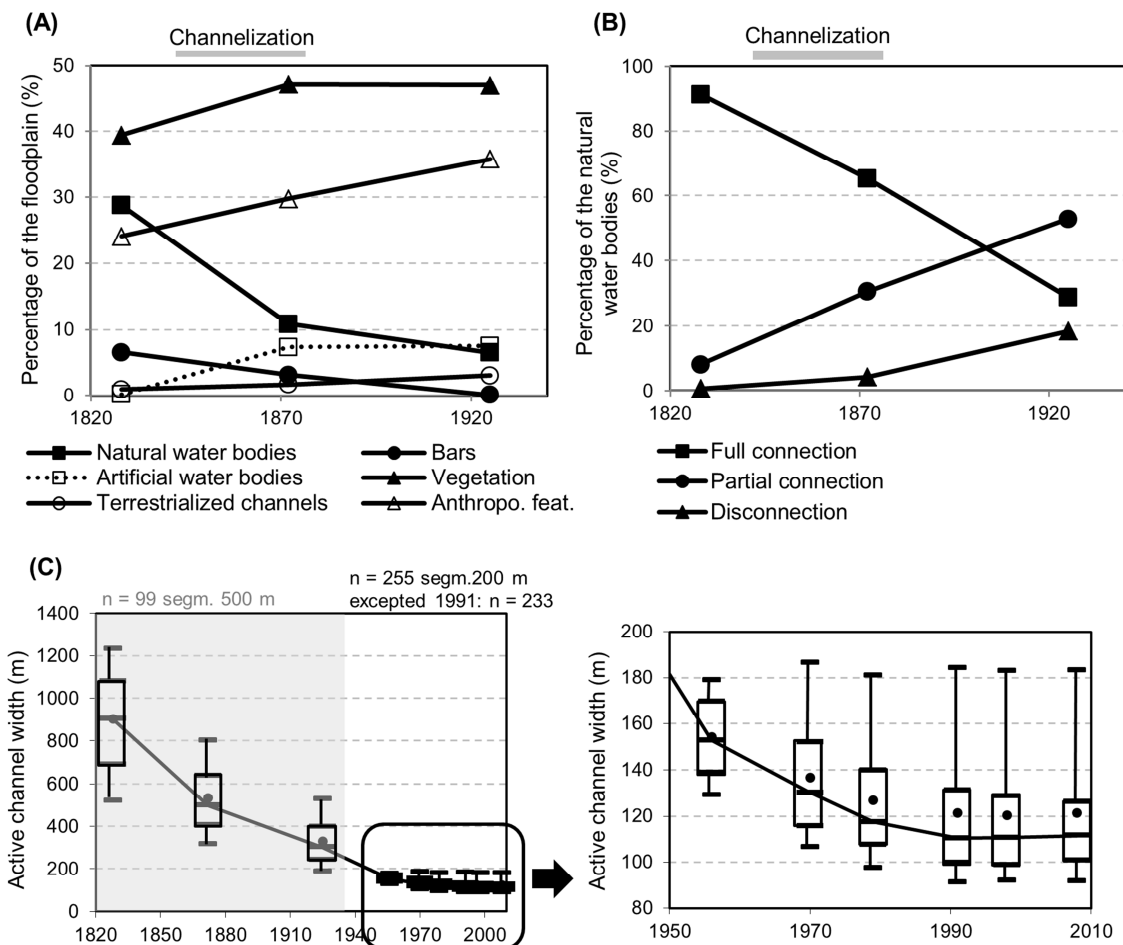
281

## 282 **4. Results**

### 283 *4.1. Planform changes (1828-2008)*

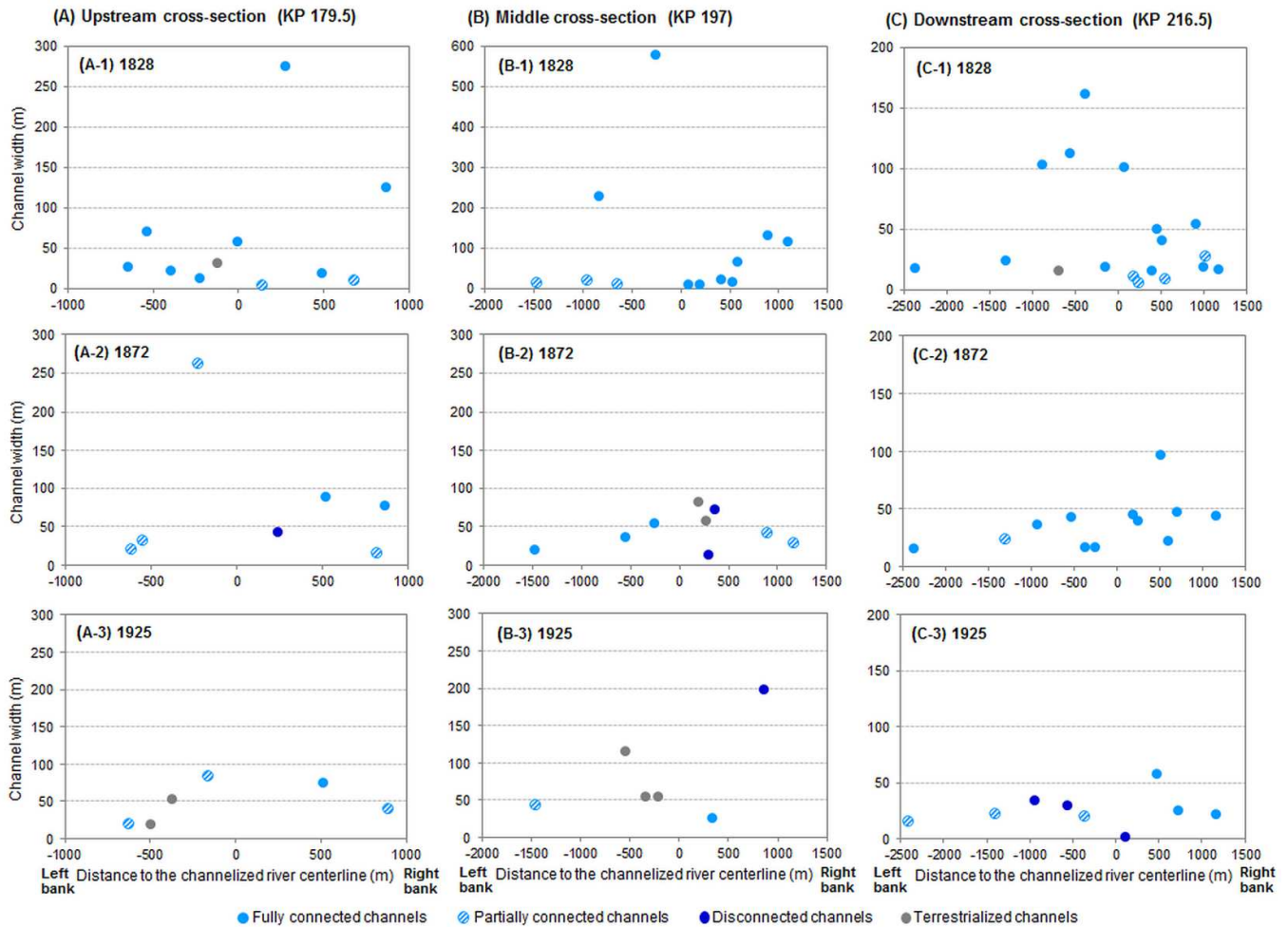
284 Prior to channelization, natural areas (water bodies, bars, vegetation, terrestrialized channels)  
285 occupied 76% of the total hydrosystem area (Fig. 4A). The remaining 24% of anthropogenic areas  
286 consisted mainly of croplands. Some high-flow dikes and local embankments (1%) were constructed  
287 at bends (see the 1828 cartography in Fig. 3), with fully connected channels being the prevalent  
288 channel type prior to channelization (91% of the area of natural water bodies; Fig. 4B).

289 Lateral analysis showed a very complex pattern with numerous channels, up to 18 on the downstream  
 290 cross section (Fig. 5C-1). The largest channels (up to 578 m wide; Fig. 5B-1) were present in the  
 291 center of the hydrosystem, while narrow channels (less than 20 m wide) were present further from the  
 292 mainstem, up to 2.4 km away (Fig. 5C-1). The thalweg lines from 1828 and 1838 were a median of  
 293 142 m distant to each other, thus highlighting the lateral channel migration prior to channelization. The  
 294 channel sinuosity was fairly constant, with median values of 1.1 and 1.2 for 1828 and 1838,  
 295 respectively; it had decreased to 1.0 in 1872. In 1828, 50% of the 5-km long segments had a sinuosity  
 296 lower than 1.0 because the hydrosystem centerline used as a reference was locally more sinuous than  
 297 the 1872 channelized river centerline.



298

299 Fig. 4. (A) Changes in fluvial and anthropogenic features related to the hydrosystem area over 1828–  
 300 1925. (B) Changes in the types of channel connection related to the area of natural water bodies over  
 301 1828–1925. (C) Changes in active-channel width over 1828–2008. Box plots provide the 10<sup>th</sup>, 25<sup>th</sup>,  
 302 50<sup>th</sup>, 75<sup>th</sup>, and 90<sup>th</sup> percentiles and mean values.



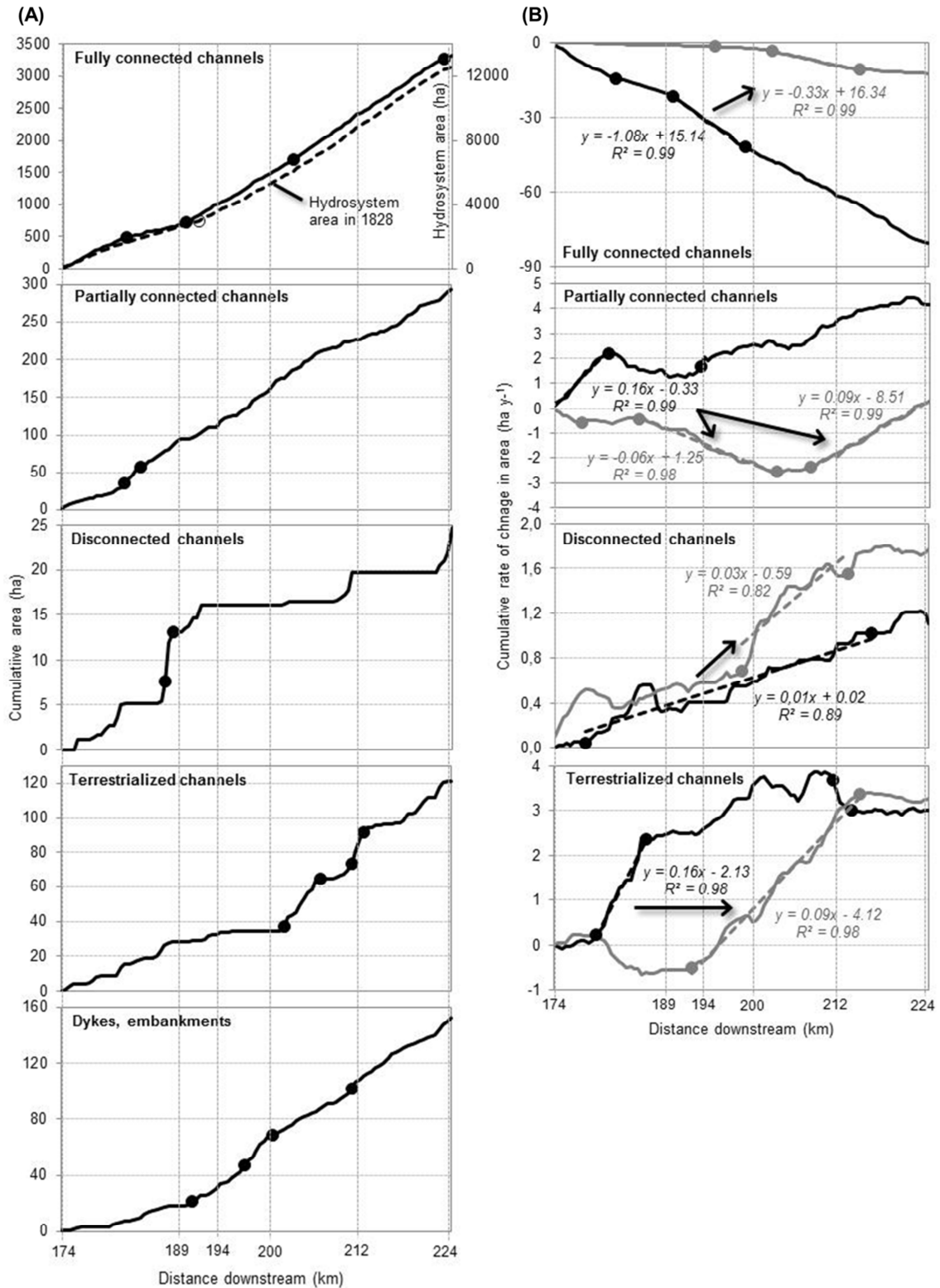
303 Fig. 5. Lateral distribution of aquatic and terrestrialized channels on three cross sections in 1828,  
 304 1872, and 1925.

305

306 The channelization induced a drastic floodplain drying out (Fig. 4A): between 1828 and 1925, natural  
 307 water bodies decreased from 29% to 7% of the total hydrosystem area, vegetated areas increased  
 308 from 39% to 47%, terrestrialized channels increased from 1% to 3%, and bars virtually disappeared  
 309 (6.6% to 0.1%). Changes in natural water bodies and vegetation were expressed mainly between  
 310 1828 and 1872, the same time period during which the augmentation of artificial water bodies  
 311 occurred. Anthropogenic features (mainly croplands) increased at a constant rate between 1828 and

1925, from 24% to 36% of the hydrosystem area. Partially connected channels became the prevalent channel type in 1925 (53% of the area of natural water bodies; Fig. 4B). Fewer channels were also present per cross section, not exceeding 13 channels in 1872 (Fig. 5C-2) and 10 channels in 1925 (Fig. 5C-3) (including disconnected water bodies). The channels also became narrower, not exceeding a width of 263 m in 1872 (Fig. 5A-2) and 197 m in 1925 (Fig. 5B-3). Channels located away in the floodplain experienced changed hydrological connectivity, from fully connected to partially connected, but were still present in 1925, contrary to most of the channels located near the mainstem (Fig. 5A-3 to 5C-3; see also maps in Fig. 3). The median active-channel width decreased from 902 to 302 m over the period 1828–1925, which is a 67% channel narrowing (Fig. 4C). Channel width then decreased further to 111 m in 2008, which gives an 88% total channel narrowing over the 181-yr period. The greatest narrowing occurred between 1828 and 1872, with a median rate of  $7.4 \text{ m yr}^{-1}$ . If we assume that narrowing was driven by channelization, then the median rate was  $10.9 \text{ m yr}^{-1}$  over the period 1842–1872. After 1956, the median rate was below  $1.3 \text{ m yr}^{-1}$ , and it became asymptotic after 1991.

The 1828 hydrosystem extent was longitudinally heterogeneous: it was narrower upstream of KP 191 and wider downstream (Fig. 6A). It controlled the longitudinal pattern of channels in 1828, with a higher fully connected channel area downstream of this point, as well as dikes and embankments aimed at stabilizing the braided and anabranching channels. Changes over 1828–1925 propagated longitudinally (see dotted regression lines and arrows in Fig. 6B): over the period 1828–1872, the reduction in fully connected channel area was the highest between KP 190 and 199 (rate of  $-1.08 \text{ ha yr}^{-1} \text{ m}^{-1}$ ). Then, over the 1872–1925 period, it was highest between KP 202.5 and 215, but at a lower rate than in the previous period ( $-0.33 \text{ ha yr}^{-1} \text{ m}^{-1}$ ). The augmentation of the terrestrialized channel area over the 1828–1872 period was the highest between KP 180 and 186.5 (rate of  $0.16 \text{ ha yr}^{-1} \text{ m}^{-1}$ ), while over the 1872–1925 period it was the highest between KP 192.5 and 215, although at a slightly lower rate than over the previous period ( $0.09 \text{ ha yr}^{-1} \text{ m}^{-1}$ ). The partially connected channel area initially increased upstream of KP 181.5 ( $0.16 \text{ ha yr}^{-1} \text{ m}^{-1}$ ), then decreased between KP 185.5 and 203 ( $-0.06 \text{ ha yr}^{-1} \text{ m}^{-1}$ ), before increasing downstream of KP 208 ( $0.09 \text{ ha yr}^{-1} \text{ m}^{-1}$ ). Finally, the area of disconnected water bodies initially increased at a low rate below KP 178.5 ( $0.01 \text{ ha yr}^{-1} \text{ m}^{-1}$ ), then increased at a higher rate than in the previous period below KP 198.5 ( $0.03 \text{ ha yr}^{-1} \text{ m}^{-1}$ ). The overall propagation rate of channel changes based on the four channel types in Fig. 6 was  $280 \text{ m yr}^{-1}$ .



341 Fig. 6. (A) Cumulative areas of the hydrosystem extent, the channel types and dikes/embankments in  
 342 a downstream direction in 1828. (B) Cumulative rates of change in area of the channel types in a  
 343 downstream direction between 1828 and 1872 (in black), and between 1872 and 1925 (in grey;

344 measured per 500-m segment; rates of changes in 1828–1872 have been calculated since the  
345 beginning of channelization (1842)). Points indicate the discontinuities detected with the Hubert test.  
346 Dotted regression lines and arrows show the downstream propagation of changes.

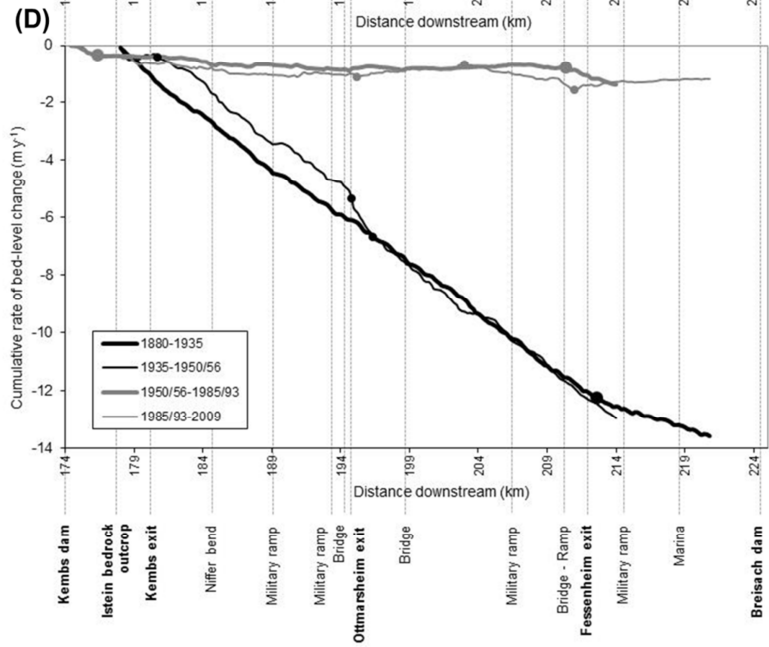
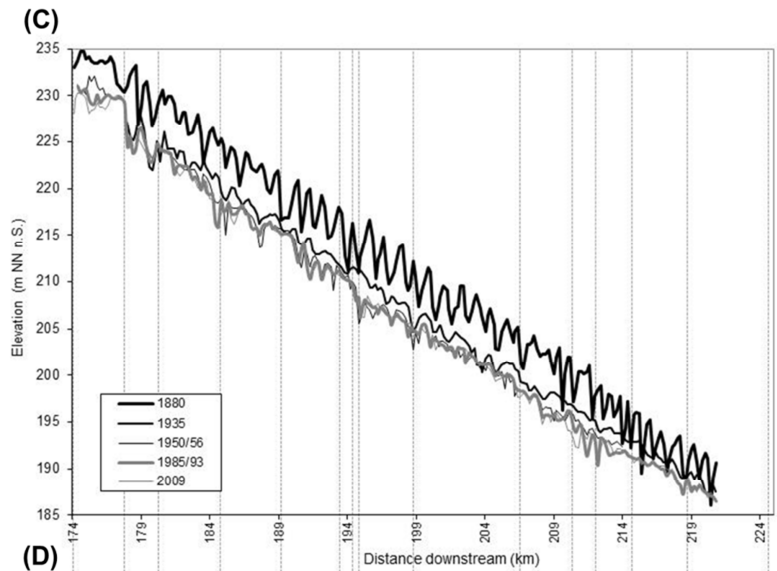
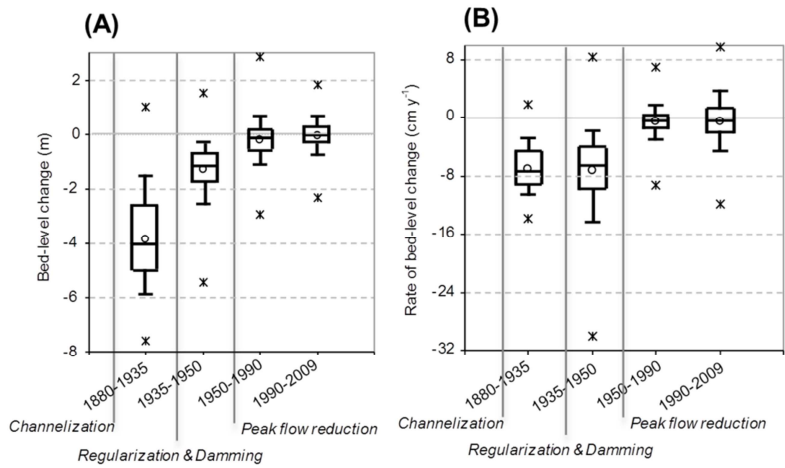
347

#### 348 *4.2. Bed-level changes (1880–2009)*

##### 349 *4.2.1. Thalweg analysis*

350 Bed-level differences indicated an intensive bed degradation between 1880 and 1950, with a median  
351 value of 4.1 m over 1880–1935 and 1.2 m over 1935–1950 (Fig. 7A), corresponding to median rates of  
352 7.4 and 6.6 cm yr<sup>-1</sup> respectively. Since the 1950s, bed degradation has stabilized at median rates of  
353 0.4 cm yr<sup>-1</sup> (1950–1985) and 0.5 cm yr<sup>-1</sup> (1985–2009) (Fig. 7B). The spatial pattern of bed degradation  
354 was longitudinally homogeneous between 1880 and 1935, except downstream of KP 212 (the future  
355 Fessenheim by-passed exit), where the process was attenuated (Fig. 7D). This spatial pattern was  
356 fairly similar between 1935 and 1950, with the exception of a drastic slowing of the process on the  
357 upstream reach (Kembs Dam to Kembs by-passed exit) and a substantial acceleration on a 1.6-km  
358 long reach immediately below the Ottmarsheim exit. After the 1950s, the slight bed-level changes  
359 occurred in homogeneous subreaches with successive trends of bed degradation, equilibrium, and  
360 bed degradation, with these remaining constant until 2009 (Fig. 7D).

361 The thalweg exhibited bed topography of large forms in 1880, with pool-riffle sequences of 4.0 m in  
362 median amplitude, locally reaching to 6.6 m (Fig. 7C). The pool-riffle amplitude had decreased  
363 drastically by 1935, with a median value of 1.1 m. It then decreased gradually until 2009 (median value  
364 of 0.8 m). The pool-riffle spacing was fairly constant between 1880 (995 m) and 1935 (990 m), but it  
365 became irregular (standard deviations of 244 m in 1880 and 424 m in 1935). The pool-riffle spacing  
366 then decreased between 1950 and 2009 (median spacing of 790–825 m; standard deviation of 332–  
367 433 m). The ratio D/W increased from values of 4.8–4.7 in 1880–1935 to 5.2 in 1950. In 1985–2009, it  
368 exceeded a value of 7 (7.5–7.2).



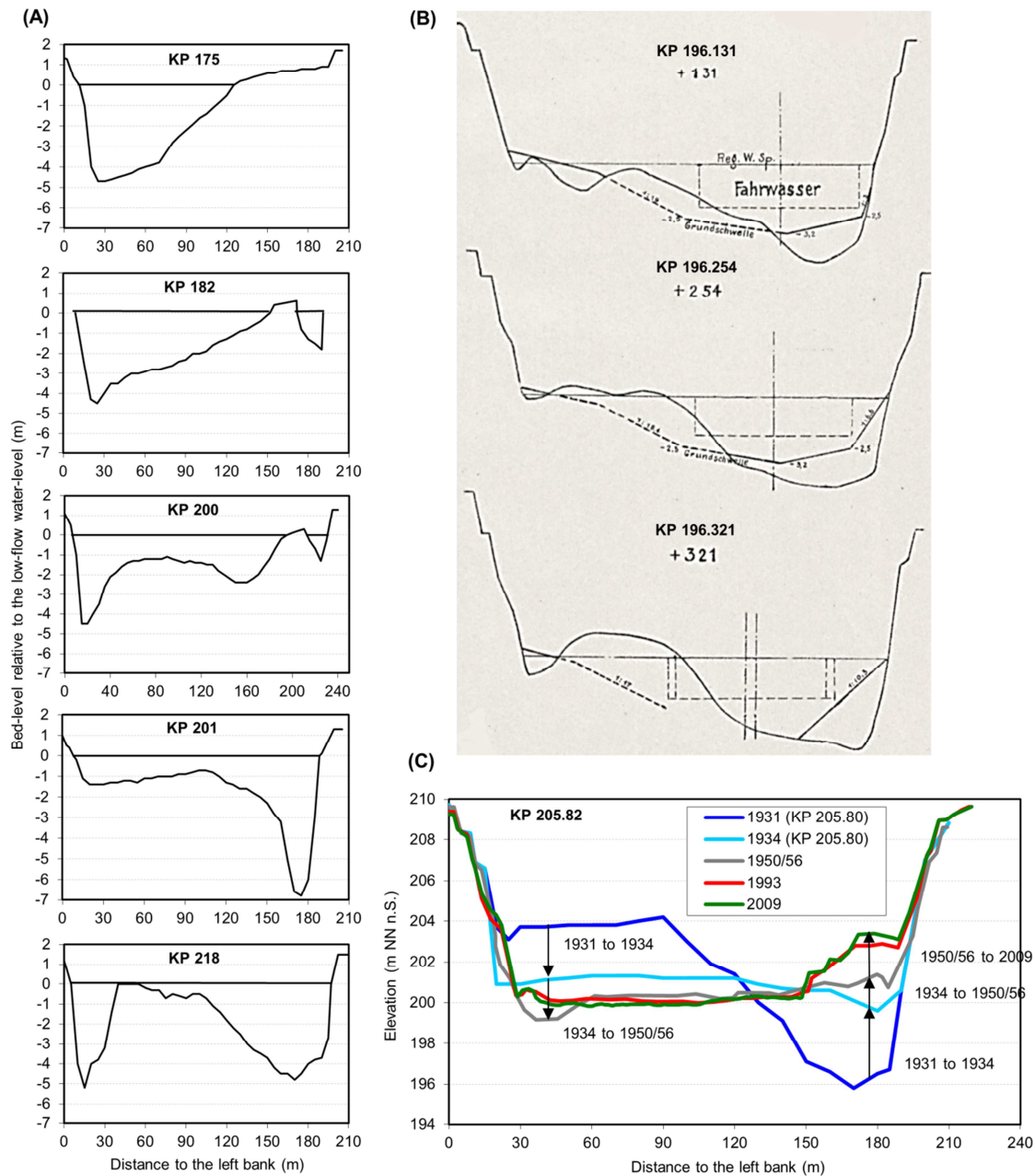
398 Fig. 7. (A) Thalweg elevation changes and (B) rates (measured every 200 m, n = 179). (C) Thalweg  
399 longitudinal profile and (D) cumulative rates of thalweg elevation change in a downstream direction.  
400 Points indicate the discontinuities detected with the Hubert test.

401

#### 402 *4.2.2. Cross-section analysis*

403 The surveys in 1884 indicated a strong heterogeneity in the geometry of the corrected channel.  
404 Among the 21 cross sections studied, all were asymmetric: 70% with one or more side channels and  
405 30% single channel with shoals or lateral bars (Fig. 8A). Among the 60 cross sections studied in 1923,  
406 60% had at least two channels and 40% had a single channel with shoals. Furthermore, the spacing of  
407 the surveys in 1923 (every 100 m along 1-km long reaches) emphasized the lateral thalweg migration  
408 (Fig. 8B).

409 Comparison of the 14 cross sections between 1930 and 2009 shows a strong simplification of the  
410 channel geometry over time. The main evolution trend was a two-channel mid-shoal bed configuration,  
411 which evolved in a single flat channel bed. Significant changes occurred in the 1930s. For example,  
412 the cross section at KP 205.82 (Fig. 8C) exhibited more changes in the three years 1931–1934 than  
413 over the twenty years 1934–1950s. The channel and the margins (groyne fields) gradually  
414 differentiated between 1950 and 2009: the channel bed was either incised or stable, and the margins  
415 aggraded on almost all the 14 cross sections. The only cross section that did not exhibit margin  
416 aggradation was located upstream of the Istein outcrop, where no groynes were built.



417 Fig. 8. Selection of cross sections showing the channel geometry (A) in 1884; (B) in 1923 (3  
 418 successive cross sections); (C) from 1931 to 2009. See Table 2 for details on data sources. Cross  
 419 sections in 1884 and 1931–2009 have been reproduced. Cross sections in 1923 are from scanned  
 420 original documents.  
 421

## 422 5. Discussion

### 423 5.1. Temporal trends and magnitudes of change

424 Prior to channelization, the Upper Rhine exhibited a highly complex braided and anabranching pattern,  
425 with numerous gravel/sand bars and extensive vegetated islands. This pattern was relatively common  
426 on large alpine rivers such as the Danube (Hohensinner et al., 2004) and the Rhône (Bravard et al.,  
427 1986). Secondary channels located near the braided mainstem were laterally active anabranches  
428 (type 5 on the Nanson and Knighton (1996) classification), as observed from the examination of the  
429 1828 and 1838 maps (see also Figs. 3 and 5). The lateral channel migration may be caused by the  
430 high frequency of flood events at the beginning of the nineteenth century (one 100-yr flood and three  
431 10-yr floods from 1817 to 1831; see Fig. 2), at a period when the bedload transport was still active and  
432 the main channel was not yet incised, and the system was therefore very responsive in the lateral  
433 dimension. High channel shifting, which was exacerbated in the active bedload transport conditions,  
434 was also observed on alpine braided rivers in France by Lallias-Tacon et al. (2017). On the Upper  
435 Rhine, the active hydrological period in the early nineteenth century could be linked to the Little Ice  
436 Age, which may have had increased the flood frequency and the associated morphodynamics  
437 (Eschbach et al., 2018). A similar phenomenon was observed by Bonnefont and Carcaud (1997) on  
438 the Moselle River (tributary of the Middle Rhine) in the eighteenth century. However, the effect of the  
439 Little Ice Age on the morphodynamics augmentation of the Upper Rhine has not yet been validated  
440 and awaits further testing (Wetter et al., 2011; Eschbach et al., 2018).

441 The study reach exhibited, on the margin of the multiple channel complex, anastomosing channels  
442 (type 1 on the Nanson and Knighton classification, 1996; see Fig. 1C). The presence of these  
443 anastomoses is referred to by *Giessen*, *Muhlbach* and *Brunnenwasser* in local literature on the Rhine  
444 (Carbiener and Dillmann, 1992). Narrow and sinuous anastomoses located farther away in the  
445 floodplain were still hydrologically connected on the 1872 and 1925 maps (Figs. 3 and 5).  
446 Anastomoses were more present in the downstream sectors of the Upper Rhine near Strasbourg  
447 (Carbiener and Schnitzler, 1990).

448 The study reach (bed slope:  $0.001 \text{ m m}^{-1}$ ) reacted very sensitively to channelization, which is in accord  
449 with several studies. On the Austrian Danube (bed slope:  $0.0005 \text{ m m}^{-1}$ ), Hohensinner et al. (2011)  
450 showed that the initial channelization phase (1821-1829) affected only 4% of the river length, but that  
451 it led to significant modifications in aquatic and riverine habitats compared with the “natural” phase

452 (before 1821). Over the following decades, the age structure of the floodplain complex was shown to  
453 be strongly correlated with the degree of channelization. On the Piave River (bed slope: 0.003–0.006  
454  $\text{m m}^{-1}$ ), Surian and Rinaldi (2003) showed an intensification of the channel narrowing process since  
455 the 1960s, linked with a major increase in bank protection structures, dams, diversions, and gravel  
456 mining since the 1950s. From a review of several Italian rivers, the authors reported short reaction  
457 times for channel narrowing and bed degradation following channelization and further river  
458 engineering.

459 On the Rhine, we found a 93% reduction in fully connected channel area, a 513% augmentation of the  
460 area of disconnected water bodies, and a 98% reduction of bar area over a 97-yr period. These  
461 changes are higher than measured on the Austrian Danube over a 179-yr period (65% reduction in  
462 fully connected channels, double-augmentation of disconnected water bodies, 94% reduction in bars;  
463 Hohensinner et al., 2004). The rate of channel narrowing on the Rhine ( $0.80\% \text{ yr}^{-1}$ ; 1842–1925) was  
464 high compared with those measured on five reaches of the channelized Lower Rhône ( $0.24\text{--}0.85\% \text{ yr}^{-1}$ ;  
465 1855–1944; Provansal et al., 2014). Additionally, the bed degradation magnitude (4.1 m in median  
466 value and 7.6 m in maximum value; 1880–1935) was in the same range or higher than a great  
467 diversity of channelized rivers in Italy (3–4 m commonly measured, with up to 10 m; Surian and  
468 Rinaldi, 2003), the Northern Alps (up to 8–14 m; Peiry et al., 1994), Poland (up to 3.1 m; Zawiejska  
469 and Wyzga, 2010), and the Mississippi River (3.5–6 m on average; higher than 10 m in a number of  
470 reaches; Hudson et al., 2008). Furthermore, the heterogeneous shape of the Rhine cross sections  
471 from the 1880s to the 1920s was similarly observed on the Isère and Arc rivers (Girel et al., 2003). On  
472 these systems, intensive morphodynamics took place after the nineteenth century river straightening,  
473 with the formation of regularly spaced (500 to 700 m) alternate bars between dikes.

474 In the two-century long temporal trajectory of the Upper Rhine, bed degradation rates following  
475 channelization ( $\sim 7 \text{ cm yr}^{-1}$ ; 1880–1950) were more than 10 times higher than after damming and by-  
476 passing ( $\sim 0.4 \text{ cm yr}^{-1}$ ; 1950–2009). Furthermore, active channel narrowing affected a wider channel  
477 system in the nineteenth century, and thus it was logically much more important following  
478 channelization ( $10.9 \text{ m yr}^{-1}$ ; 1842–1872) than following damming and by-passing (1.3 to  $0.1 \text{ m yr}^{-1}$ ;  
479 1956–2008; see Arnaud et al., 2015 for details of the post-damming temporal trajectory).

480 Groynes had no effect on the bed degradation rate, which has remained constant since  
481 channelization. However, groynes rapidly simplified the cross-sectional geometry and induced a

482 significant decrease in the pool-riffle spacing. The decrease in the pool-riffle spacing continued after  
483 damming and by-passing. The values of  $D/W$  (4.7–7.5) are consistent with the literature on pool-riffle  
484 geometry (5–7; Leopold et al., 1964; Gregory et al., 1994). Interestingly, the ratio  $D/W$  increased  
485 during the studied period, especially since the 1990s (4.7–5.2 between 1880 and 1950; higher than  
486 7.0 between 1990 and 2009), when the active channel was narrower with vegetation encroachment on  
487 the dewatered groyne fields. An increase in  $D/W$  following channelization and damming was described  
488 by Gregory et al. (1994) in a review of several case studies.

489 Bed grain size surveys performed in 2011 indicated that partial bed armoring (armoring degree  
490 between 1.1 and 2.1) developed after channelization (Arnaud et al., 2015). This could explain why the  
491 sediment loss calculated in the by-passed Old Rhine ( $550 \text{ m}^3 \text{ km}^{-1} \text{ yr}^{-1}$ ; 1990–2010; Arnaud et al.,  
492 2015) was much lower than measured on the by-passed Rhône at Chautagne ( $1250 \text{ to } 1450 \text{ m}^3 \text{ km}^{-1}$   
493  $\text{yr}^{-1}$ ; 1970–1980; Klingeman et al., 1998). This reach of the Upper Rhône did not undergo  
494 channelization prior to damming, and the riverbed is not armored. This may explain the higher  
495 sediment loss and bed incision rates.

496 Channelization was the most impactful engineering phase in terms of planform and vertical changes  
497 on the Upper Rhine. Similarly, on the Lower Rhône (Provansal et al., 2014), much of the geomorphic  
498 change occurred several decades prior to the 1950s damming and 1970s gravel mining, as a joint  
499 consequence of channelization in the mid-nineteenth century and the overall reduction in sediment  
500 input from the Rhône basin. With regard to the long-term timescale of the Upper Rhine, Kock et al.  
501 (2009) found that the highest level of the Lower Terrace (accumulation surface) in the area of Basel is  
502 approximately 30 m higher than the present Rhine level. The Lower Terrace was thus incised by about  
503 30 m within not more than 12 ka, which represents a mean incision rate of  $2.5 \text{ mm yr}^{-1}$  (Kock et al.,  
504 2009). In the present study, channelization thus increased the bed incision process by a factor of 28 ( $7$   
505  $\text{cm yr}^{-1}$ ). This can be explained by the narrower channel geometry without flow reduction, which  
506 increased the hydraulic competence without any possibility of lateral erosion. It therefore drastically  
507 increased incision of the river bottom. In contrast, damming was the engineering phase with the most  
508 impact on peak flows. The frequency with which the critical discharge for bedload entrainment was  
509 exceeded ( $Q_c = 550 \text{ m}^3 \text{ s}^{-1}$ ) was reduced by a factor of 22 following damming (Arnaud et al., 2015).  
510 This can explain the lower magnitude of channel changes in the most recent period.

511

512 *5.2. Spatial patterns and linkages between planform and bed-level changes*

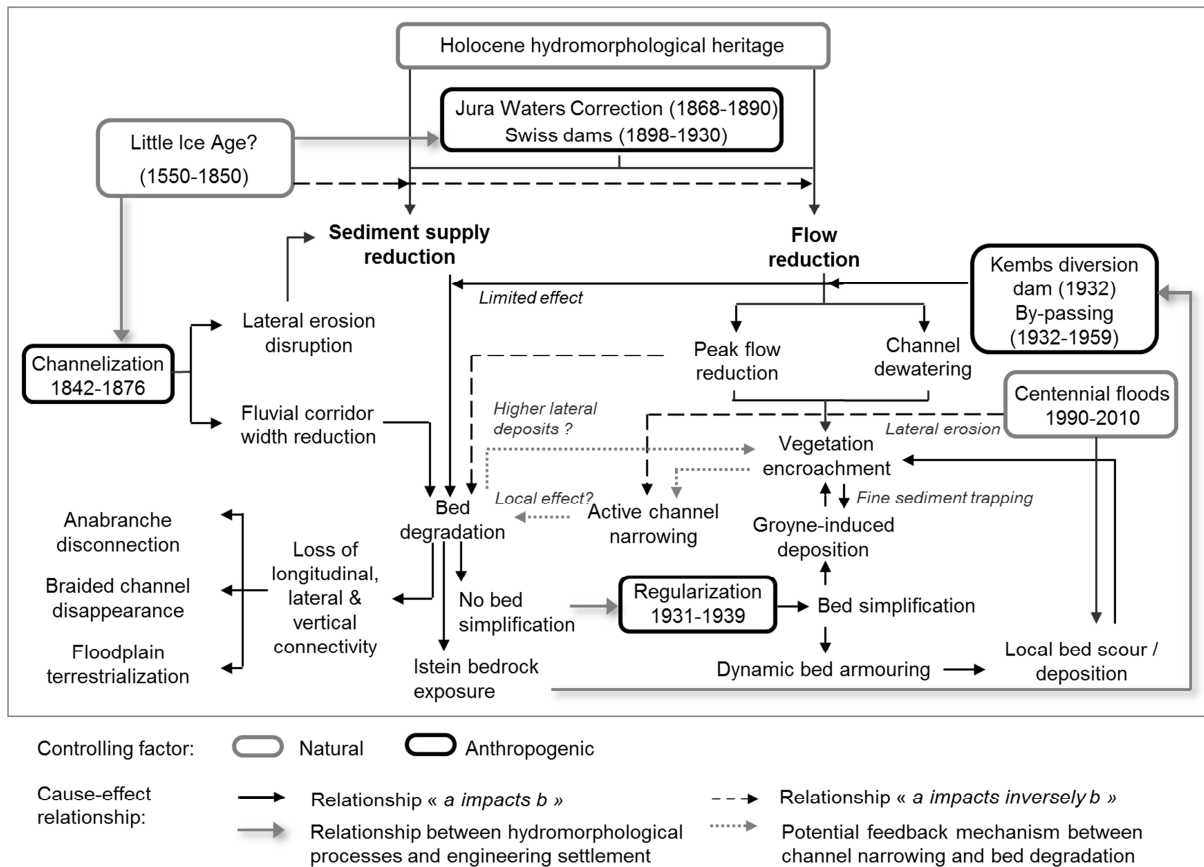
513 We found the longitudinal pattern of channel adjustments over time to be somewhat complex,  
514 depending on the channel type and the spatial arrangement of the channels prior to channelization  
515 (Fig. 6). Side channels continued to evolve after channelization, as seen on the 1925 map, meaning  
516 that the relaxation period for adjustment to the new straightened river pattern covered several decades  
517 after the works were completed. The overall propagation rate of channel changes ( $280 \text{ m yr}^{-1}$ ) is  
518 slightly lower than those found in the literature for a watershed reforestation context (French Southern  
519 Prealps streams:  $300$  to  $500 \text{ m yr}^{-1}$ ; Liébault et al., 2005) or damming context (Ain River, tributary of  
520 the French Rhône:  $\sim 500 \text{ m yr}^{-1}$ ; Rollet et al., 2014). The rivers in these studies were affected by  
521 different anthropogenic disturbances; however, the higher rates could also be explained by higher  
522 energy river systems and closer sediment sources. On the study reach, the spatial pattern of channel  
523 adjustments could be controlled by bed degradation, which decreased the hydrological connectivity  
524 between the main channel and its floodplain both vertically and laterally. Some studies demonstrated  
525 lowering of the groundwater level based on historical piezometric records on small sectors of the  
526 Upper Rhine (records for 1828–1955 in the Harth forest, Gendrin et al., 1957; records for 1907–1938  
527 near Ottmarsheim, Simler et al., 1979). However, water-level records showed a higher rate of  
528 decrease on the upstream reach of the Upper Rhine, which then propagated downstream (CHR, 1977,  
529 p.148): between 1828 and 1880, the change in the water level reached a maximum rate of  $-4 \text{ cm yr}^{-1}$   
530 at KP 186 (approaching  $-3 \text{ cm yr}^{-1}$  at KP 199.5), then between 1880 and 1920 this maximum was  $-9$   
531  $\text{cm yr}^{-1}$  at KP 199.5 (approaching  $-8 \text{ cm yr}^{-1}$  at KP 186). The change in water level was less  
532 pronounced downstream of KP 215, with a rate of  $-3$  and  $-7 \text{ cm yr}^{-1}$  over the two periods. This result  
533 is consistent with our comparison of thalweg profiles between 1880 and 1935, which showed that bed  
534 degradation was attenuated downstream of KP 212 (Fig. 7C). Therefore, information on planform and  
535 vertical changes over the nineteenth–early twentieth century seems to validate the hypothesis that the  
536 longitudinal pattern of floodplain drying out was controlled by the longitudinal pattern of bed  
537 degradation.

538 The bed degradation process differed in the downstream reaches of the Upper Rhine. For example,  
539 the change in water level was only  $-1 \text{ cm yr}^{-1}$  (1828-1880) at Strasbourg, which is located 125 km  
540 downstream of our study reach (CHR, 1977). Eschbach et al. (2018) reported a 70% reduction of bar  
541 area and a 50% reduction of connected channel area on the 4-km long Rohrschollen island near

542 Strasbourg (1833-1876), which are less than the values of 98% and 81%, respectively, on our study  
543 reach (1828-1925). Diaz-Redondo et al. (2017) studied changes in habitat structure on a 10-km long  
544 reach near Iffezheim, which is located 160 km downstream of our study reach. This reach firstly  
545 exhibited bed degradation ( $-3 \text{ cm yr}^{-1}$ ; 1828-1880), then bed aggradation resulting from the upstream  
546 bedload supply ( $+1 \text{ cm yr}^{-1}$ ; 1880-1920) (CHR, 1977). The authors found lower magnitudes of  
547 floodplain drying out (1830–1930), with fully connected channels decreasing from 33% to 12% of the  
548 floodplain area (versus 26% to 2% on our study reach; 1828-1925), partially connected channels  
549 increasing from 3% to 8% (versus 2% to 3%), and disconnected water bodies increasing from 1% to  
550 2% (versus 0.7% to 18%). Downstream attenuation of the bed degradation process was observed on  
551 the Rhône downstream of Lyon (Parrot, 2015), with bed degradation being very intense in the first  
552 kilometers of the channelized reach (Pierre-Bénite reach; 1897-1953). This reach changed into a more  
553 effective bedload transport configuration because of the bed incision, without upstream bedload input;  
554 thus, it was assumed to have fed the downstream reaches and limited the downstream propagation of  
555 the sediment deficit. On the Rhine, if the magnitude of planform and vertical changes decreased  
556 downstream, the transformation of gravel bars and islands into vegetation or agricultural land following  
557 channelization was observed all along the Upper Rhine continuum (Basel to Lauterburg; 185-km long)  
558 by Ricaurte et al. (2012), similar to the changes exhibited on the Upper Danube (Austria-Slovakia) and  
559 Olt River (Romania).

560 Following this study and the findings of Arnaud et al. (2015), we synthesized the channel adjustments  
561 in the study reach over the past 200 yr (Fig. 9). Complex cause-effect relationships between  
562 natural/anthropogenic controlling factors and hydromorphological processes took place in the 3.5-km  
563 wide multiple channel system, then in the 200-m wide channelized river. The effects of long-term  
564 (Holocene and Little Ice Age heritage) and basin-scale (Swiss engineering works) drivers on the two  
565 controlling variables of the fluvial system (the sediment supply and the flow regime) were also  
566 indicated. Interestingly, hydromorphological processes lasting several decades had further impact on  
567 engineering settlement (solid grey arrows in Fig. 9). For example, the 1930s groyne field construction  
568 took place to stabilize the long profile because the nineteenth century channelization increased flow  
569 velocity and gravel bar mobility, which complicated navigation between Germany and Switzerland. The  
570 damming and by-passing schemes were initiated at the same period, not only for hydroelectric  
571 purposes, but also because the Istein bedrock outcrop could not be crossed by boats on 332 days per

572 year in the 1920s, and the construction of a lateral canal was needed (Humbert and Descombes,  
 573 1985).

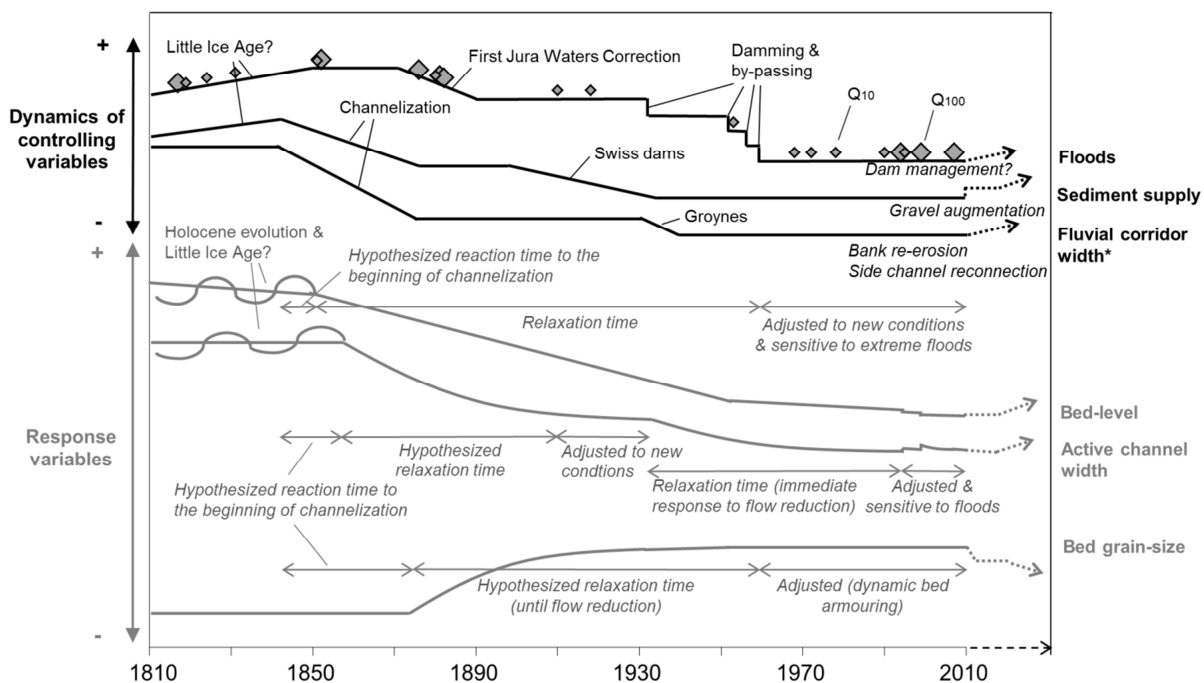


574 Fig. 9. Synthesis of the Upper Rhine channel adjustments to natural and anthropogenic controlling  
 575 factors over the past 200 yr. This figure describes cause-effect relationships “a impacts b” (solid black  
 576 arrows), “a inversely impacts b” (dotted black arrows), and “impacts of hydromorphological processes  
 577 on engineering settlement” (solid grey arrows) demonstrated during this study. The potential feedback  
 578 mechanism between active channel narrowing and bed degradation (dotted grey arrows) was  
 579 discussed by Arnaud et al. (2015).

580

581 5.3. Implications for river restoration

582 This historical analysis showed that the Upper Rhine followed a non-linear evolutionary trend over the  
 583 last two centuries (Fig. 10). The flood regime, sediment supply, and fluvial corridor width changed  
 584 either progressively or in steps. These changes were either permanent, such as channelization, or  
 585 temporary, such as floods (Dufour and Piégay, 2009). The responses of the geomorphic variables  
 586 were either synchronous or were assumed to be delayed. Thresholds were reached in the adjustments  
 587 of the bed-level, active-channel width, and bed grain-size. Currently, the system seems adjusted to the  
 588 new conditions of the controlling variables, but its morphology remains sensitive to floods (Arnaud et  
 589 al., 2015). This model provides a knowledge framework with which river restoration scenarios can be  
 590 discussed.



591 Fig. 10. Controlling variables (in black) and response variables (in grey) of channel morphodynamics  
 592 over the past 200 yr. The bed grain-size trend information is from Arnaud et al. (2015). Dotted arrows  
 593 indicate the potential river restoration trends. The ordinate axis is in relative units.

594 \*The fluvial corridor width is the artificially constrained width in which most of the flow runs (e.g.: the  
 595 200-m wide corridor following channelization; the 75-m wide corridor following regularization). It differs  
 596 from the active-channel width because some channels and gravel bars were still remnant outside the  
 597 embankments. The fluvial corridor width is indicated as a controlling variable because it was directly  
 598 modified by anthropogenic activities, such as floods and sediment supply.

599

600 The present-day challenges for the Old Rhine are to increase bedform mobility to create hydraulic and  
601 habitat diversity based on artificial gravel augmentation (Arnaud et al., 2017), and to allow bank re-  
602 erosion through dike removal (Chardon et al., 2017). Such strategies, if implemented on a large scale,  
603 would move the evolutionary trends of the response variables towards a more dynamic system (see  
604 dotted arrows in Fig. 10). Our retrospective analysis of side channels has helped to specify the nature  
605 of changes (e.g., changes in hydrological connectivity, vegetation, or cropland) and their spatial and  
606 temporal magnitudes (Fig. 6). This is critical information for identifying sites for functional channel  
607 restoration and determining their sustainability. In 2013, a 7-km long former channel was reconnected  
608 to the Old Rhine, immediately below the Kembs Dam (Reynier et al., 2015). This is a first encouraging  
609 measure, because the possibilities for former channel restoration are very limited given the intense  
610 floodplain artificialization on the study reach. The downstream reaches of the Upper Rhine are also  
611 highly urbanized, but they are less incised (see Section 4.2); thus, floodplain channel restoration is  
612 more feasible (Diaz Redondo et al., 2017; Eschbach et al., 2018). Another encouraging large-scale  
613 program concerns flood control on the whole of the Upper Rhine (Integrated Rhine Programme; Kuhn  
614 et al., 2016). On the German side of the Old Rhine, the floodplain surface is being lowered to create  
615 flood retention areas of up to 25 million m<sup>3</sup> capacity. By enhancing lateral connectivity in these  
616 retention areas, the aim is also to improve the mosaic of biotopes in the Rhine floodplain (Kuhn et al.,  
617 2016).

618

## 619 **6. Conclusion**

620 This study provides new insights on the long-term (181 yr) trajectory of a large multi-impacted braided  
621 and anabranching river. Among the three phases of engineering works that affected the Upper Rhine  
622 (channelization, groyne construction, damming), channelization had the most impact on planform  
623 (floodplain terrestrialization, end of channel shifting) and vertical (intensive bed degradation) changes,  
624 with a short reaction time and effects over several decades. Damming had the most impact on peak  
625 flows, which explains the lower magnitude of channel changes in the most recent period. The complex  
626 pattern of a 50-km long continuum of the Rhine floodplain prior to major pressures has been quantified  
627 for the first time, as well as the downstream propagation of the changes. The present Old Rhine  
628 follows an evolutionary trend inherited from the nineteenth century, but is adjusted to the controlling  
629 variables imposed by damming since the 1950s, especially peak flood reduction, which decreased the

630 frequency of critical flows for bedload transport. Finally, the nature and magnitude of the changes in  
631 side channels, which are here quantified in space and time, are critical contributions to the  
632 understanding of large braided and anabranching multi-impacted rivers in a functional restoration  
633 context.

634

### 635 **Acknowledgements**

636 This research was supported by the European Regional Development Fund within the project  
637 “Redynamization of the Old Rhine” (FEDER INTERREG IV Upper Rhine) and by Electricité de France  
638 within the research collaboration “Sediment reintroduction into the Old Rhine from controlled bank  
639 erosion”. We thank Dorothée Hoenen for GIS assistance and Karl Embleton for proof-reading. Finally,  
640 we thank the two reviewers for their comments that substantially improved the quality of this  
641 manuscript.

642

### 643 **References**

- 644 Arnaud, F., Piégay, H., Schmitt, L., Rollet, A.J., Ferrier, V., Béal, D., 2015. Historical geomorphic  
645 analysis (1932-2011) of a by-passed river reach in process-based restoration perspectives: the  
646 Old Rhine downstream of the Kembs diversion dam (France, Germany). *Geomorphology* 236,  
647 163–177.
- 648 Arnaud, F., Piégay, H., Béal, D., Collery, P., Vaudor, L., Rollet A.J., 2017. Monitoring gravel  
649 augmentation in a large regulated river and implications for process-based restoration. *Earth*  
650 *Surf. Process. Landforms* 42(13), 2147–2166.
- 651 Bonnefont, J.C., Carcaud, N., 1997. The morphodynamic behaviour of Moselle River before its  
652 harnessings. *Géomorphologie: relief, processus, environnement* 3(4), 339–353.
- 653 Bornette, G., Amoros, C., Rostan, J.C., 1996. River incision and decennial vegetation dynamics in cut-  
654 off channels. *Aquat. Sci.* 58(1), 31–51.
- 655 Bravard, J.P., Bethemont, J., 1989. Cartography of rivers in France. In: Petts, G.E., Moller, H., Roux,  
656 A.L. (Eds.), *Historical Change of Large Alluvial Rivers: Western Europe*. John Wiley & Sons,  
657 Chichester, pp. 95–111.
- 658 Bravard, J.P., Gaydou, P., 2015. Historical development and integrated management of the Rhône  
659 River floodplain, from the Alps to the Camargue Delta, France. In: Hudson, P.F., Middelkoop, H.



690 Diaz-Redondo, M., Egger, G., Marchamalo, M., Hohensinner, S., Dister, E., 2017. Benchmarking  
691 fluvial dynamics for process-based river restoration: the Upper Rhine River (1816–2014). *River*  
692 *Res. Applic.* 33, 403–414.

693 Downs, P.W., Gregory, K.J., 2004. *River Channel Management. Towards Sustainable Catchment*  
694 *Hydrosystems*. Arnold, London.

695 Dufour, S., Piégay, H., 2009. From the myth of a lost paradise to targeted river restoration: forget  
696 natural references and focus on human benefits. *River Res. Applic.* 25(5), 568–581.

697 Eschbach, D., Schmitt, L., Imfeld, G., May, J.H., Payraudeau, S., Preusser, F., Trauerstein, M.,  
698 Skupinski, G., 2018. Long-term temporal trajectories to enhance restoration efficiency and  
699 sustainability on large rivers: an interdisciplinary study. *Hydrol. Earth Syst. Sci.* 22, 2717–2737.

700 Frings, R.M., Gehres, N., Promny, M., Middelkoop, H., Schüttrumpf, H., Vollmer, S., 2014. Today's  
701 sediment budget of the Rhine River channel, focusing on the Upper Rhine Graben and Rhenish  
702 Massif. *Geomorphology* 204, 573–587.

703 Gendrin, P., Millot, G., Simler, L., 1957. Etude de la nappe phréatique de la plaine du Haut-Rhin.  
704 *Mémoires du Service de la carte géologique d'Alsace et de Lorraine* 15, 40 p. (in French).

705 Ghezzi, C., 1926. Die Abflussverhältnisse des Rheins in Basel. Bern: Eidg. Departement des Innern  
706 (in German).

707 Girel, J., Vautier, F., Peiry, J.L., 2003. Biodiversity and land use history of the alpine riparian  
708 landscapes (the example of the Isère River valley, France). In: Mander, U., Antrop, M. (Eds.),  
709 *Multifunctional Landscapes, Volume 3: Continuity and Change*. WIT-Press, Southampton, pp. 167–  
710 200.

711 Gregory, K.J., 2006. The human role in changing river channels. *Geomorphology* 79, 172–191.

712 Gregory, K.J., Gurnell, A.M., Hill, C.T., Tooth, S., 1994. Stability of the pool-riffle sequence in changing  
713 river channels. *Regul. Rivers Res. Manag.* 9, 35–43.

714 Gregory, S., Ashkenas, L., Oetter, D., Minear, P., Wildman, K., 2002. Historical Willamette River  
715 Channel Change. In: Hulse, D., Gregory, S., Baker, J. (Eds.), *Willamette River Basin Planning*  
716 *Atlas*. Oregon State University Press, Corvallis, pp. 18–25.

717 Herget, J., Eckhard, B., Coch, T., Dix, E., Eggenstein, G., Ewald, K., 2005. Engineering impact on river  
718 channels in the River Rhine catchment. *Erdkunde* 59, 294–319.

719 Hohensinner, S., Habersack, H., Jungwirth, M., Zauner, G., 2004. Reconstruction of the characteristics  
720 of a natural alluvial river-floodplain system and hydromorphological changes following human  
721 modifications: the Danube River (1812-1991). *River Res. Applic.* 20, 25–41.

722 Hohensinner, S., Jungwirth, M., Muhar, S., Schmutz, S., 2011. Spatio-temporal habitat dynamics in a  
723 changing Danube River landscape 1812—2006. *River Res. Applic.* 27, 939–955.

724 Hubert, P., 2000. The segmentation procedure as a tool for discrete modeling of hydrometeorological  
725 regimes. *Stoch. Environ. Res. Risk Assess.* 14, 297–304.

726 Hudson, P.F., Middelkoop, H., Stouthamer, E., 2008. Flood management along the Lower Mississippi  
727 and Rhine Rivers (The Netherlands) and the continuum of geomorphic adjustment.  
728 *Geomorphology* 101, 209–236.

729 Humbert, J., Descombes, R., 1985. Rhin. *Encyclopédie de l'Alsace*, Strasbourg, pp. 6391–6400 (in  
730 French).

731 Klingeman, P.C., Bravard, J.P., Giuliani, Y., Olivier, J.M., Pautou, G., 1998. Hydropower reach by-  
732 passing and dewatering impacts in gravel-bed rivers. In: Klingeman, P.C., Beschta, R.L., Komar,  
733 P.D., Bradley, J.B. (Eds.), *Gravel Bed Rivers in the Environment*. Water Resources Publications,  
734 Littleton, pp. 313–344.

735 Kock, S., Huguenberger, P., Preusser, F., Kramers, J.D., Wetzel, A., 2009. Formation and evolution of  
736 the Lower Terrace of the Rhine River in the area of Basel. *Swiss J. Geosci.* 102(2), 307–321.

737 Kuhn, S., Migenda, W., Pfarr, U., 2016. *The Integrated Rhine Programme. Flood control and*  
738 *restoration of former floodplains along the Upper Rhine*. Ministry of the Environment, Climate  
739 Protection and the Energy Sector, Stuttgart, 11 p.

740 Lallias-Tacon, S., Liébault, F., Piégay, H., 2017. Use of airborne LiDAR and historical aerial photos for  
741 characterising the history of braided river floodplain morphology and vegetation responses.  
742 *Catena* 149(3), 742–759.

743 Leopold, L.B., Wolman, M.G., Miller, J.P., 1964. *Fluvial Processes in Geomorphology*. Freeman, San  
744 Francisco.

745 Liébault, F., Gomez, B., Page, M., Marden, M., Peacock, D., Richard, D., Trotter, C.M., 2005. Land-  
746 use change, sediment production and channel response in upland regions. *River Res. Applic.* 21,  
747 739–756.

748 Mika, S., Hoyle, J., Kyle, G., Howell, T., Wolfenden, B., Ryder, D., Keating, D., Boulton, A., Brierley,  
749 G., Brooks, A., Fryirs, K., Leishman, M., Sanders, M., Arthington, A., Creese, R., Dahm, M., Miller,  
750 C., Pusey, B., Spink, A., 2010. Inside the “black box” of river restoration: using catchment history  
751 to identify disturbance and response mechanisms to set targets for process-based restoration.  
752 *Ecology and Society* 15(4), 20 p.

753 Nanson, G.C., Knighton, A.D., 1996. Anabranching rivers: their cause, character and classification.  
754 *Earth Surf. Process. Landforms* 21, 217–239.

755 Nivière, B., Giamboni, M., Innocent, C., Winter, T., 2006. Kinematic evolution of a tectonic wedge  
756 above a flat-lying décollement: The Alpine foreland at the interface between the Jura Mountains  
757 (Northern Alps) and the Upper Rhine graben. *Geology* 34(6), 469–472.

758 Parrot, E., 2015. Analyse spatio-temporelle de la morphologie du chenal du Rhône du Léman à la  
759 Méditerranée. Ph.D. Thesis, Université Lyon 3, France (in French).

760 Peiry, J.L., 1986. Dynamique fluviale historique et contemporaine du confluent Giffre-Arve (Haute-  
761 Savoie). *Revue de géographie de Lyon* 61(1), 79–96 (in French).

762 Peiry, J.L., Salvador, P.G., Nougier, F., 1994. L'incision des rivières dans les Alpes du nord : état de  
763 la question. *Revue de géographie de Lyon* 69(1), 47–56 (in French).

764 Piégay, H., Alber, A., Slater, L., Bourdin, L., 2009. Census and typology of braided rivers in the French  
765 Alps. *Aquat. Sci.* 71, 371–388.

766 Pišút, P., 2002. Channel evolution of the pre-channelized Danube River in Bratislava, Slovakia (1712–  
767 1886). *Earth Surf. Process. Landforms* 27, 369–390.

768 Provansal, M., Dufour, S., Sabatier, F., Anthony, E., Raccasi, G., Robresco, S., 2014. The geomorphic  
769 evolution and sediment balance of the lower Rhône River (southern France) over the last 130  
770 years: Hydropower dams versus other control factors. *Geomorphology* 219, 27–41.

771 Reynier, T., Lachat, B., Morand, D., Steinle, A., Barillier, A., Garnier, A., 2015. Restoration of an old  
772 bed of the river Rhine on the Kembs island: Innovative processes and tools in an ambitious site's  
773 service. ISRivers Conference. Abstract 2B33-49443REY.

774 Ricaurte, L.F., Boesch, S., Jokela, J., Tockner, K., 2012. The distribution and environmental state of  
775 vegetated islands within human-impacted European rivers. *Freshwater Biology* 57, 2539–2549.

776 Rollet, A.J., Piégay, H., Dufour, S., Bornette, G., Persat, H., 2014. Assessment of consequences of  
777 sediment deficit on a gravel river bed downstream of dams in restoration perspectives: application  
778 of a multicriteria, hierarchical and spatially explicit diagnosis. *River Res. Applic.* 30, 939–953.

779 Roux, C., Alber, A., Bertrand, M., Vaudor, L., Piégay, H., 2015. “FluvialCorridor”: A new ArcGIS  
780 toolbox package for multiscale riverscape exploration. *Geomorphology* 242, 29–37.

781 Schmitt, L., Houssier, J., Martin, B., Beiner, M., Skupinski, G., Boës, E., Schwartz, D., Ertlen, D.,  
782 Argant, J., Gebhardt, A., Schneider, N., Lasserre, M., Trintafillidis, G., Ollive, V., 2016. Paléo-  
783 dynamique fluviale holocène dans le compartiment sud-occidental du fossé rhénan (France).  
784 *Revue Archéologique de l’Est* 42, 15–33 (in French).

785 Schneider, G., 1966. Zusammenfassende darstellung der Rheinregulierung Strassburg/Kehl-Istein.  
786 Baukommission des Unternehmens “Regulierung des Rheins zwischen Strassburg/Kehl und  
787 Istein”. Freiburg (in German).

788 Scorpio, V., Surian, N., Cucato, M., Dai Prá, E., Zolezzi, G., Comiti, F., 2018. Channel changes of the  
789 Adige River (Eastern Italian Alps) over the last 1000 years and identification of the historical fluvial  
790 corridor. *J. Maps* 14(2), 680–691.

791 Simler, L., Valentin, J., Duprat, A., 1979. La nappe phréatique de la plaine du Rhin en Alsace. Institut  
792 de Géologie, Université Louis Pasteur, Strasbourg (in French).

793 Surian, N., Rinaldi, M., 2003. Morphological response to river engineering and management in alluvial  
794 channels in Italy. *Geomorphology* 50, 307–326.

795 Tricart, J., Bravard, J.P., 1991. Le cours périalpin du Rhin, du Rhône et du Danube: aménagement  
796 fluvial et dérives de l’environnement. *Annales de Géographie* 561-562, 668–713 (in French).

797 Tulla, J.G., 1825. Mémoire sur la rectification du cours du Rhin. *Journal de la Société des Sciences,*  
798 *Agriculture et Arts de Strasbourg*, pp. 5–69 (in French).

799 Uehlinger, U., Wantzen, K.M., Leuven, R.S.E.W., Arndt, H., 2009. The Rhine River basin. In: Tockner,  
800 K., Uehlinger, U., Robinson, C.T. (Eds.), *Rivers of Europe*. Elsevier, London, pp. 199–246.

801 Vetter, T., 2011. Riffle-pool morphometry and stage-dependant morphodynamics of a large floodplain  
802 river (Vereinigte Mulde, Sachsen-Anhalt, Germany). *Earth Surf. Process. Landforms* 36, 1647–  
803 1657.

804 Walser, E., 1959. Le bassin du Rhin à l’amont de Bâle et l’influence des lacs sur le régime du fleuve.  
805 *La Houille Blanche* 2, 115–124 (in French).

- 806 Wetter, O., Pfister, C., Weingartner, R., Luterbacher, J., Reist, T., Trösch, J., 2011. The largest floods  
807 in the High Rhine basin since 1268 assessed from documentary and instrumental evidence.  
808 Hydrol. Sci. J. 56(5), 733–758.
- 809 Zawiejska, J., Wyżga, B., 2010. Twentieth-century channel change on the Dunajec River, southern  
810 Poland: Patterns, causes and controls. Geomorphology 117(3–4), 234–246.
- 811 Ziliani, L., Surian, N., 2016. Reconstructing temporal changes and prediction of channel evolution in a  
812 large Alpine river: the Tagliamento River, Italy. Aquat. Sci. 78, 83–94.